

Integrating Biomimetic Synergy with Linkage-Driven Mechanisms: An Anthropomorphic Hand for Versatile Grasping and Manipulation

Hao Wu, Zhaohui Lin, Yanzhe Wang, Haotian Guo, and Huixu Dong[†]

Abstract—The human hand, renowned for its unparalleled dexterity and adaptability, has long served as the quintessential model for robotic hand design. However, replicating the intricate biomechanics of the human hand while maintaining its lightweight and compact structure remains a significant challenge. Existing humanoid hands emerge with several limitations, including high cost and structural complexity, limited dexterity, and inadequate sensory feedback. To address these research gaps, this study investigates the synergistic characteristics of human hand movements and integrates them with advanced linkage-driven mechanisms to develop a novel anthropomorphic dexterous hand. First, we perform biomechanical analysis to quantitatively capture joint angles during various grasping and manipulation tasks using sensor gloves, identifying key synergistic movements and providing a reasonable basis for structural simplification. Second, we design planar linkage mechanisms that effectively replicate synergy-based coupled joint motions while ensuring the structural compactness of the hand. Through structural optimization, the kinematic performance of these mechanisms is refined to closely emulate natural human hand gestures. Third, a spatial linkage mechanism is introduced to facilitate the motion of a two-degree-of-freedom (2-DOF) joint. This structure enables efficient motion transmission for power grasping within confined spaces while fully decoupling lateral and flexion movements, allowing for independent actuation of each DOF. A series of experimental evaluations are conducted to demonstrate the hand’s versatility in grasping diverse objects, manipulating tools for specialized tasks, and performing precise actions in practical applications. In conclusion, this study presents a viable solution for designing compact, high-performance robotic hands with a simplified configuration, effectively bridging the gap between mechanical complexity and functional capability.

Index Terms—Anthropomorphic hand, linkage-driven mechanism, biomimetic analysis, structural optimization, tool operation

I. INTRODUCTION

THE human hand is widely recognized as one of the most complex parts of the human body, serving as a critical medium for object manipulation and tactile interaction. Its high degree of freedom and multimodal sensory feedback endow it with remarkable flexibility and adaptability in complex grasping tasks. From multi-fingered [1], [2] grippers to anthropomorphic hands [3], classic design approaches have consistently endeavored to replicate the appearance and dexterity of human hands with sophisticated mechanisms integrating more actuators and sensors. However, significant challenges remain in seeking perfect structural and functional anthropomorphism, resulting in limited real-world applications.

The concept of hand synergy from neuroscience [4], [5] provides a promising approach to reducing this complexity

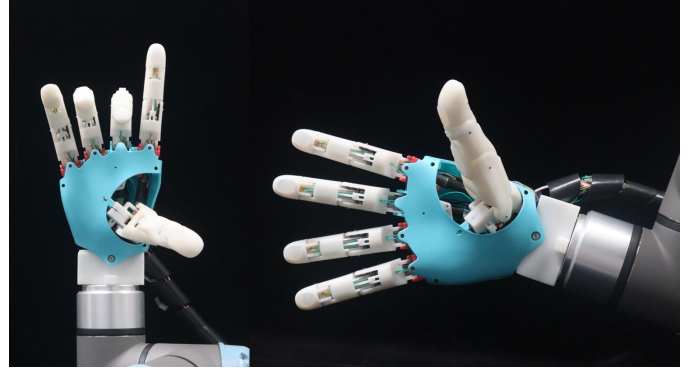


Fig. 1. The prototype of the dexterous hand with an appearance and functionality akin to that of the human hand.

without compromising dexterity. Extensive related studies have been conducted to deepen our understanding of the hand’s grasping strategies, synergistic characteristics, and methodologies for translating these insights into robotic hand design. For instance, Chen et al. [6] applied principal component analysis (PCA) to motion data obtained using sensor gloves and proposed a universal design theory for prosthetic hands. By leveraging the identified key biomechanical synergies, the prototype X-hand, actuated by only four motors, demonstrated the capability to perform 91% of daily human grasping activities. Similarly, Sun [7] presented a robotic hand powered by just two actuators, capable of replicating a wide range of human grasping gestures through independent thumb movement and synergistic finger actions. Additionally, this concept has shown strong practicality in the design of task-specific robotic hands. Inspired by efficient swing mechanics, Chang [8] developed an anthropomorphic prosthetic hand designed specifically for sports activities. It incorporates human anatomical features and tendon routing to enhance swing efficiency, enabling amputees to achieve a 19% increase in swing speed. Karnati [9] investigated human finger synergies during screwing and unscrewing motions, and subsequently developed sinusoidal joint trajectories that allowed a robotic hand to perform analogous tasks with a single input. Although the complexity reduction brought by the synergistic organization in these designs enables the replication of most human grasping capabilities or specific tasks, the inherent limitation in degrees of freedom restricts their application in more complex manipulation and general operation tasks.

The integrity and versatility of robotic hands largely depend

To design an anthropomorphic hand capable of human-like grasping and manipulation, it is necessary to set up a reasonable experimental paradigm for obtaining the dataset of human hand movements. This dataset provides fundamental insights into the kinematic mechanisms and synergistic characteristics of manual dexterity. In this experiment, we used the Quantum Mocap Metagloves (MANUS) to quantitatively capture the joint angles of the human hand during grasping tasks involving objects of various shapes and sizes, performed in the subject's natural manner (Figure 2). The experimental procedure began with participants resting their hands on a tabletop, with their fingers fully extended in a relaxed state. Subsequently, they were instructed to grasp and manipulate the target objects in their usual manner, performing each task three times to minimize random errors. The experimental samples selected for the study were everyday objects and tools, chosen to cover a wide range of grasping patterns. Throughout the grasping actions, the Metagloves recorded the angular measurements of 20 joints. All measured joint angles formulate the human hand movement dataset Q for the grasping activities.

After acquiring the human hand movement dataset, we can quantitatively analyze the synergistic principles between joints and the digits. Principal component analysis (PCA) is frequently adopted to extract the fundamental synergies in human hand gestures, aiding in the analysis and optimization of the configuration of DOFs in dexterous hands [6], [9], [16], [17]. However, this approach inherently neglects the physical constraints of mechanical components, rendering the translation of these primitives into tangible mechanical structures highly complex in practical applications. Therefore, in this study, we propose an approach to analyze and extract the anatomical and functional relationships among the 20 joints of the human hand. Given that dexterous hand movements are more easily coupled between adjacent joints, we computed the correlation coefficients directly using Pearson's correlation coefficient (PCC) for these physically connected and functionally interactive joints. The PCC is calculated using the following formula, resulting in a 20×20 correlation matrix R :

$$Cov(Q_i, Q_j) = \frac{(Q_i - \bar{Q}_i)^T (Q_j - \bar{Q}_j)}{n - 1} \quad (1)$$

$$\sigma_i = \sqrt{\frac{(Q_i - \bar{Q}_i)^T (Q_i - \bar{Q}_i)}{n - 1}} \quad (2)$$

$$r_{i,j} = \frac{Cov(Q_i, Q_j)}{\sigma_i \sigma_j} \quad (3)$$

For non-adjacent joints, the correlation coefficients are derived by sequentially multiplying the correlation coefficients of the intermediate adjacent joints along the path connecting them in the hand's anatomical structure. This approach is based on the physiological principle that joint influence propagates through adjacent joints, offering a biologically plausible approximation of their functional interdependence. Hence, the propagation matrix P provides a comprehensive representation of the synergistic relationships between the hand joints. It can be obtained through the following calculation:

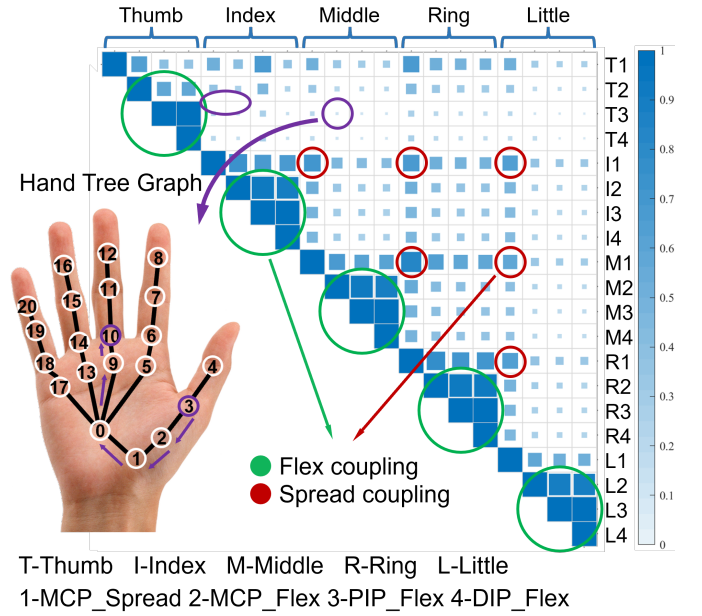


Fig. 3. Cooperativity among joints of the hand during object manipulation and grasp.

$$P_{i,j} = \begin{cases} 1 & i = j \mid i = 0, j \equiv 1 \pmod{4} \\ r_{i,j} & |i - j| = 1, 4k - 4 < i, j \leq 4k \\ r_{i,i-1} r_{i-1,j} & i - j > 1, 4k - 4 < i, j \leq 4k \\ r_{i,0} r_{j,0} r_{i_0,j_0} & j \leq 4k < i, k_0 = 4 \lfloor \frac{k-1}{4} \rfloor + 1 \end{cases} \quad (4)$$

As illustrated in Figure 3, the intensity of the line color and the size of the markers in the matrix visually encode the magnitude of correlation coefficients. This analysis reveals that the metacarpophalangeal (MCP), proximal interphalangeal (PIP), and distal interphalangeal (DIP) joints, as well as the joints involved in the lateral movements of the four fingers, exhibit strong functional coupling. These correlation patterns align with empirical observations of natural human kinematics, where these joints often function in a coordinated manner. In contrast, the thumb exhibits relatively independent kinematic behavior, reflecting its unique anatomical and functional role in grasping and manipulation tasks. These biomechanical insights have significant implications for the design of dexterous robotic hands. Hence, in the next section, we focus on the simplification and implementation of these identified joint couplings to mimic natural hand functionality. The original coupling data derived from this analysis will inform the optimization of robotic hand structural parameters, ensuring functional efficiency and mechanical feasibility.

III. MECHANISM DESIGN

A. Hand Mechanism

This dexterous hand is designed to replicate the anatomical structure, appearance, and functionality of the human hand, enabling effective grasping and manipulation. It consists of a palm and five articulated fingers, with 19 joints driven by 11 independent actuators. The general 3D model and spatial arrangement are shown in Figure 4. The hand demonstrates

mechanical efficiency with dimensional parameters of approximately 240 mm (length) \times 110 mm (width) \times 60 mm (depth) and a lightweight construction weighing 520 g. Individual fingers can generate a force output of up to 10 N, while the overall hand can sustain a maximum payload exceeding 25 N.

To achieve precise motion control and enable the generation of complex, coupled movement trajectories, linkage mechanisms are extensively employed in the design [18]. These mechanisms ensure the coordination of multiple joints while maintaining structural compactness. Furthermore, the integration of pressure and angular sensors within the finger assemblies enables real-time monitoring of force and positional data during movement. The actuation, transmission, and sensing subsystems are all integrated within the hand, contributing to its compactness, efficiency, and structural flexibility.

B. Fingers Mechanism

This design capitalizes on the anatomical similarity of the four fingers (excluding the thumb) to streamline both the manufacturing process and associated costs by implementing an identical structural design for each. The fingers are strategically positioned at varying heights on the palm to replicate the natural alignment of the human hand. As aforementioned, the motion of PIP and DIP joints demonstrates a strong linear correlation, allowing for efficient coupling. A crossed four-bar mechanism [10] is employed by interconnecting multiple segments to achieve coordinated motion between these joints. To avoid undesired coupling between the MCP and PIP joint movements and to maximize the available internal space within the finger, the actuator is placed inside the proximal phalanx. The motor's motion is transmitted to the connecting rod through a worm gear system, thereby achieving a compact structure that allows for self-locking of the position.

The thumb, being the most dexterous and powerful digit of the human hand, plays a critical role in enabling stable and effective grips by opposing the other fingers [19]. Due to its unique structure and position, the thumb necessitates a distinct design compared to the other fingers. The human thumb, characterized by its two exposed joints, is enabled by the first metacarpal bone to perform a variety of movements including rotation and flexion, thereby meeting requirements for diverse grasping and manipulation tasks. Therefore, to preserve the reconfigurable relationship between the thumb and the palm, a three-joint structure is implemented. The lateral movement adjusts the relative position between the thumb and palm, while flexion facilitates natural grasping motion. The dual degrees of freedom allow the thumb to follow a motion trajectory within a conical workspace, enabling it to contact each of the other fingers to achieve a pinch posture. Specifically, the flexion movement is driven by a motor within the base joint, which actuates the stacked crossed four-bar linkage for coordinated motion across the three joints. Meanwhile, lateral movement is facilitated by a servo motor fixed inside the palm, which drives a planar four-bar mechanism.

For linkage-driven mechanisms, the motion relationship between two adjacent joints is determined by the geometric parameters of the link. The schematic diagram of the linkage

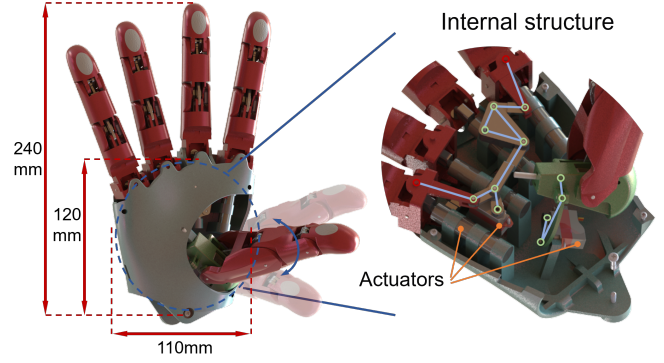


Fig. 4. Demonstration of the hand's overall structure.

mechanism is depicted in Figure 5B. To quantitatively assess its kinematic performance, the complex linkage assembly can be simplified into a four-bar linkage mechanism. l_p is the driven linkage that can control the angle of θ , while γ represents the rotation angle of the distal phalanx. With the known lengths of l_1 , l_2 , l_p , and l_c , the motion angles between the joint can be calculated:

$$l_m = \sqrt{l_1^2 + l_p^2 - 2l_1l_p\cos(\alpha + \theta)} \quad (5)$$

$$\phi = \cos^{-1}\left(\frac{l_m^2 + l_p^2 - l_1^2}{2l_ml_p}\right) \quad (6)$$

$$\phi + \theta + \gamma = \cos^{-1}\left(\frac{l_m^2 + l_2^2 - l_c^2}{2l_ml_2}\right) \quad (7)$$

$$\gamma = \cos^{-1}\left(\frac{l_m^2 + l_2^2 - l_c^2}{2l_ml_2}\right) - \cos^{-1}\left(\frac{l_m^2 + l_p^2 - l_1^2}{2l_ml_p}\right) - \theta \quad (8)$$

The kinematic performance of linkage mechanisms is critically dependent on the geometric parameters, which directly determine the trajectory and precision of the end-effector movement. To achieve optimal grasping performance and desired motion trajectories, we employed the Particle Swarm Optimization (PSO) algorithm, a robust method for handling complex, nonlinear optimization problems involving multiple linkage parameters. Specifically, the optimization framework was designed to satisfy multiple kinematic constraints while maximizing the mechanism's performance metrics. The subsequent part provides a detailed account of the solution.

1) *Objective Function*: The kinematic data acquired from hand movements provides an optimal basis for the optimization of the mechanism. The primary objective is to design a four-bar linkage system that accurately replicates the coupled motion patterns of human finger joints while adhering to predefined constraints. The optimization criterion is established through the minimization of Euclidean distance between the reference joint angles and the corresponding linkage angles, expressed mathematically as:

$$\min f(x) = \sum_{i=1}^n (\text{coupled } \theta_i - \text{target } \theta_i)^2 \quad (9)$$

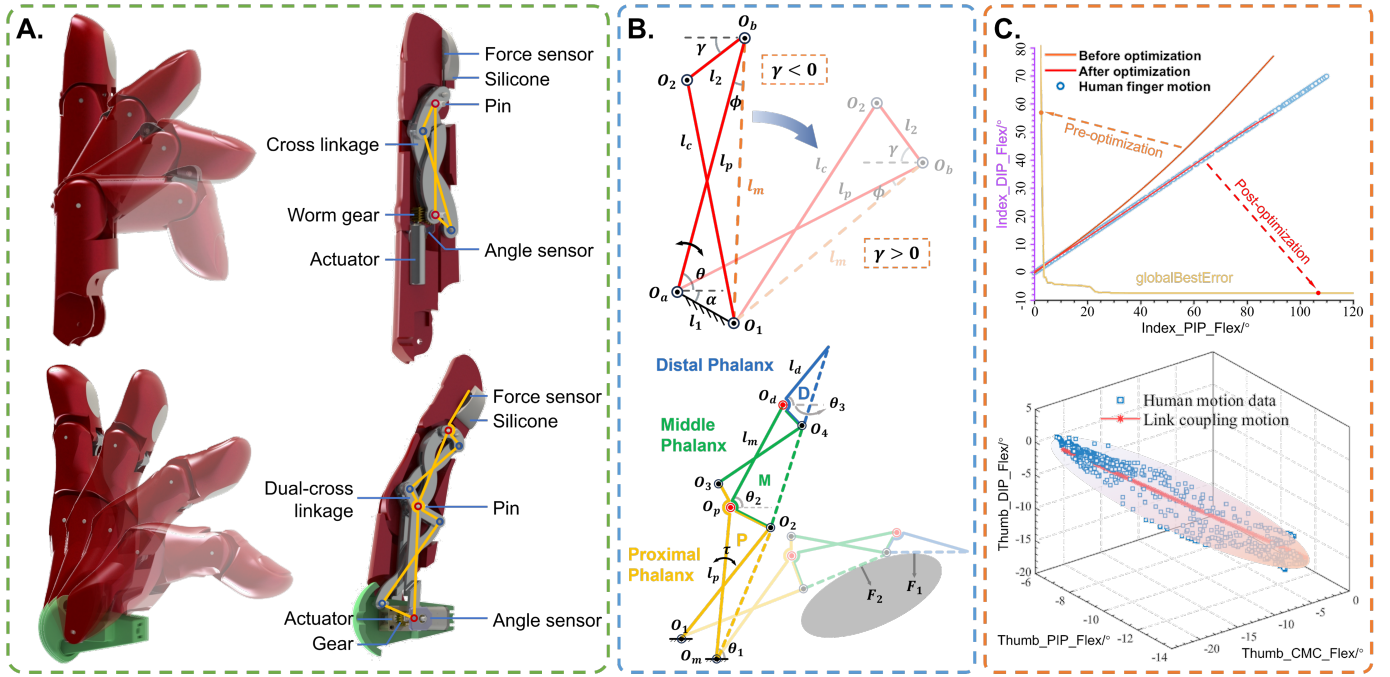


Fig. 5. Demonstration of the dexterous hand's finger structure. (A) Illustration of the finger structure and its constituent components. (B) Schematic representation of the proposed finger design. (C) Optimization results of the linkage mechanisms.

2) *Constraints*: To ensure the practical feasibility and anatomical compatibility of the mechanism, dimensional constraints were implemented based on anthropometric measurements of human fingers. The mechanism design is subject to the following fundamental constraints:

- **Grashof's condition**: The sum of the lengths of the shortest and longest links must be less than the sum of the lengths of the remaining two links to ensure continuous relative motion.
- **Dimensional boundaries**: Both link lengths and angular ranges are constrained within physiologically feasible limits to maintain anatomical realism.

3) *Results*: The optimization results, illustrated in Figure 5C, highlight the efficacy of the PSO algorithm in addressing the multi-parametric design problem. The achieved global minimum error validates the robustness of the optimization approach. As depicted by the blue scatter points, the motion among different joints shows a strong linear correlation, reflecting the inherent kinematic coupling observed in the human hand. Comparative analysis of pre- and post-optimization trajectories reveals that the linkage parameters optimized by the PSO algorithm, specifically in terms of position, length, and angular configuration, achieve a close replication of the natural motion patterns in human digits.

C. Coordinated Lateral Motion Mechanism

Although human fingers can perform abduction and adduction movements (Abd/Add) independently, such motions are rarely used during activities in daily living (ADL). Most of the time, all fingers abduct and adduct simultaneously [11], [20]. As indicated from biomechanical analysis, the index,

middle, ring, and little fingers tend to exhibit synchronized motion in natural movements. Moreover, given that the middle finger shows significantly less pronounced lateral movement compared to other digits, it is rigidly fixed to the palm in this design. Therefore, based on these physiological insights and with the objective of reducing structural complexity, a planar linkage mechanism is employed, enabling coordinated lateral movement of the index, ring, and little fingers towards or away from the middle finger with a single degree of freedom.

The transmission mechanism for Abd/Add motion is depicted in Figure 6A. A micro servo motor (KST/X06) embedded within the palm actuates the motion of the mechanism. On the side of the ring and little fingers, the motor's output is transmitted through a planar four-bar linkage mechanism connected to the base joint of the little finger. The base joint of the ring finger is mechanically coupled to that of the little finger, forming an equivalent four-bar linkage. This arrangement ensures synchronous lateral movement of both digits in response to motor actuation. The index finger, which requires opposite directional movement, is connected through a triangular linkage coupled with connecting rods, effectively forming a five-bar linkage system comprising two stacked four-bar linkages. By optimizing the lengths of the linkages, this design emulates natural human finger Abd/Add patterns, enabling coordinated three-finger lateral movement with a single actuator. At maximum abduction, the little finger exhibits the greatest articulation angle ($\approx 25^\circ$), while the index and ring fingers reach a similar range of motion angles ($\approx 15^\circ$).

Notably, the lateral motion of the index finger plays a critical role in stabilizing and supporting grasped objects. Here, to enhance this functionality, the linkage mechanism is specifically designed with a large forward transmission angle

(δ), ensuring efficient torque transmission from the actuator to the finger. Conversely, the reverse transmission angle (η) is minimized to provide mechanical resistance against external displacement forces. This strategic configuration effectively creates a mechanical locking mechanism that maintains finger position under load, thus enhancing stability and reliability during grasping and manipulation tasks.

D. Spatial Spherical Four-bar Mechanism

The incorporation of Abd/Add movements introduces significant complexity to the spatial relationship between the base joint and the motor's output shaft responsible for flexion. Consequently, conventional transmission methods, such as spur gears or worm gears, are insufficient for maintaining meshing transmission across varying lateral positions. To address this challenge, a specialized mechanism capable of accommodating two independent degrees of freedom is required.

To achieve fully decoupled bidirectional motion for both flexion and abduction of the MCP joint, we propose a four-bar spherical linkage mechanism. This mechanism, illustrated in Figure 6B, comprises an offset block and a connecting bar, forming a compact linkage chain. Unlike traditional solutions such as universal joints and differential gear mechanisms [13], which tend to be bulky and ill-suited for constrained spaces, the spherical four-bar mechanism offers a simple, compact solution that allows for greater flexibility in movement configuration. The orthogonal rotational axes allow for completely independent actuation of flexion and abduction movements, which is challenging to realize with conventional mechanisms. Upon actuation, the motor's rotational motion is transmitted to the offset block, which subsequently modulates the inclination angle of the connecting link. The finger joint, mounted on the upper surface of the connecting link, performs controlled flexion and extension movements. The schematic diagram of the structure is shown in Figure 6D. The kinematic relationship can be mathematically derived from its geometric constraints, as expressed in Equation (10):

$$\cos \alpha \cos \varphi_s \cos \beta_s + \sin \alpha \sin \beta_s = \cos \alpha \quad (10)$$

Here, φ_s denotes the input rotation angle of the motor, β_s denotes the output rotation angle of the finger joint, and α represents the fixed angle of the connecting rod.

Kinematic analysis reveals that the finger joint's flexion angle exhibits a proportional relationship with the motor's rotational angle, achieving a maximum flexion of approximately 60°. The mechanism exhibits nonlinear characteristics in its motion and torque transmission, as illustrated in Figure 6C. During the movement phase, the torque remains relatively low, while in the grasping phase, the torque increases significantly. This nonlinear characteristic is particularly advantageous for power grasping, as it aligns with the functional demands where minimal torque suffices for positioning, while substantial torque is necessary for maintaining stable object retention.

E. Integrated sensors

The perception system integrated into our dexterous hand is designed to provide comprehensive real-time feedback regarding the hand's kinematic state and its interaction with external

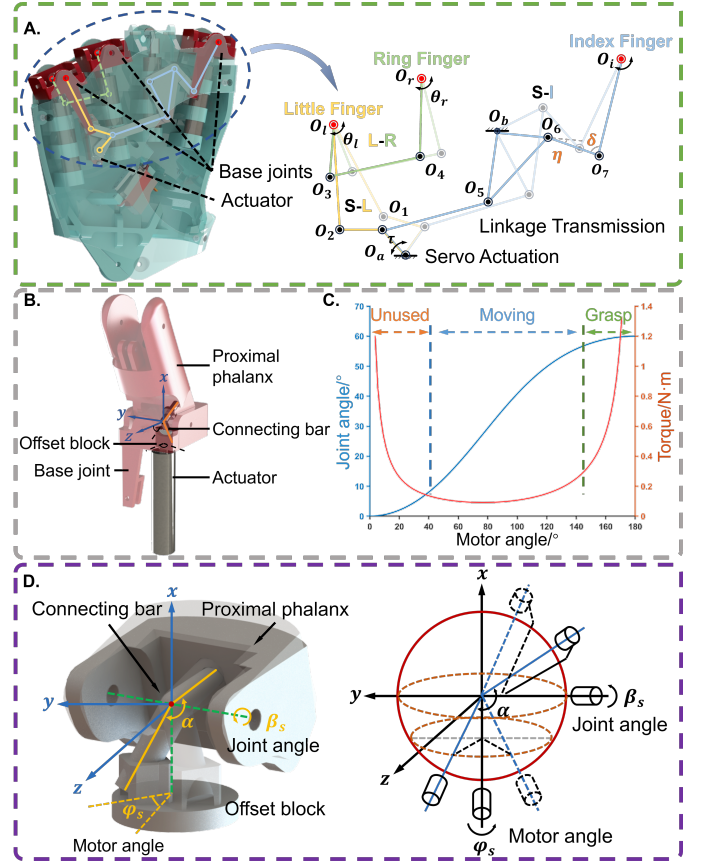


Fig. 6. Two-degree-of-freedom joint structure. (A) Coordinated lateral motion mechanism. (B) Spherical four bar linkage structure. (C) Nonlinear characteristic of the mechanism for angle and torque. (D) Structural diagram of the spatial linkage mechanism.

objects. Specifically, rotation angle sensors are embedded at each finger joint to continuously monitor joint angular positions. For joints actuated by motors with encoders, angular displacement data is acquired through temporal integration of encoder signals. This setup ensures precise joint angle measurement and close-loop control over finger movements, contributing to the coordination control of the hand's movements, particularly in complex manipulation tasks.

Complementing the sensing capabilities, our dexterous hand incorporates force sensors within the fingertip. These sensors are designed to measure the interaction forces between the hand and objects, providing essential feedback on the contact conditions. Specifically, force sensing resistors (FSR) and polyvinylidene fluoride (PVDF) film sensors are employed and embedded within the distal phalanx, with the external surface coated in silicone to ensure compliant contact with objects and enhance frictional interaction. The FSRs are primarily responsible for measuring static forces, while the PVDF sensors capture dynamic pressure variations due to their high-frequency response characteristics. With this configuration, the fingertip can not only quantify static forces but also identify surface textures and contact points. The force data obtained from the fingertips is integrated into the real-time control system, allowing the hand to adjust its grip force and posture to maintain stable and secure interaction with objects.

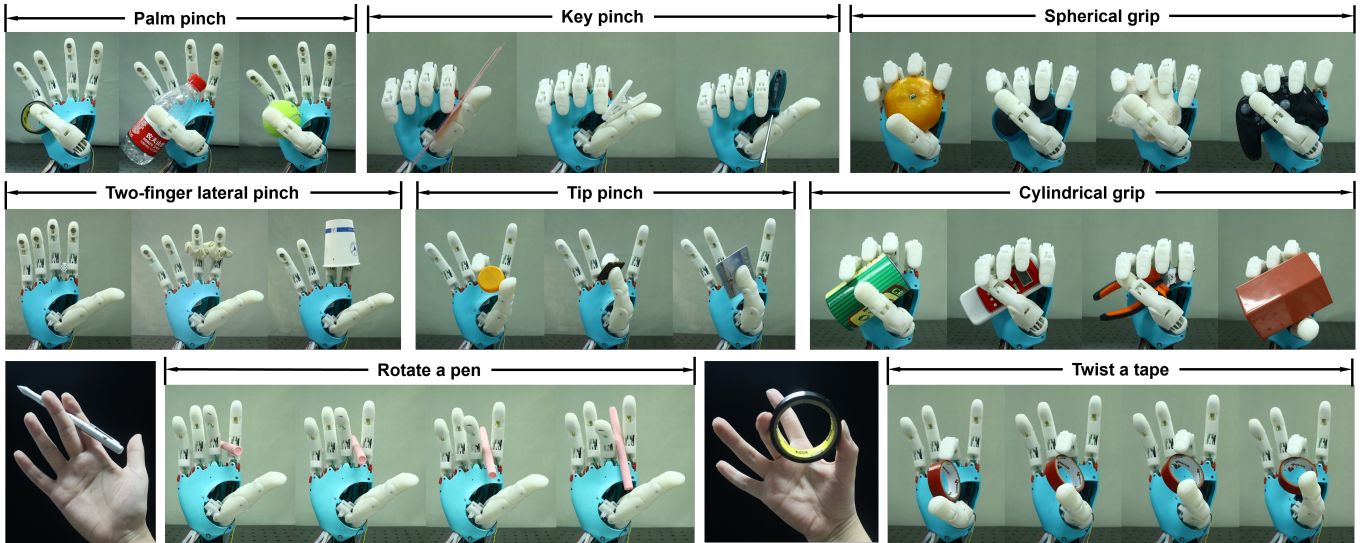


Fig. 7. Several demonstrations validate the grasping capabilities for a variety of objects and showcase manipulation skills through in-hand object repositioning.

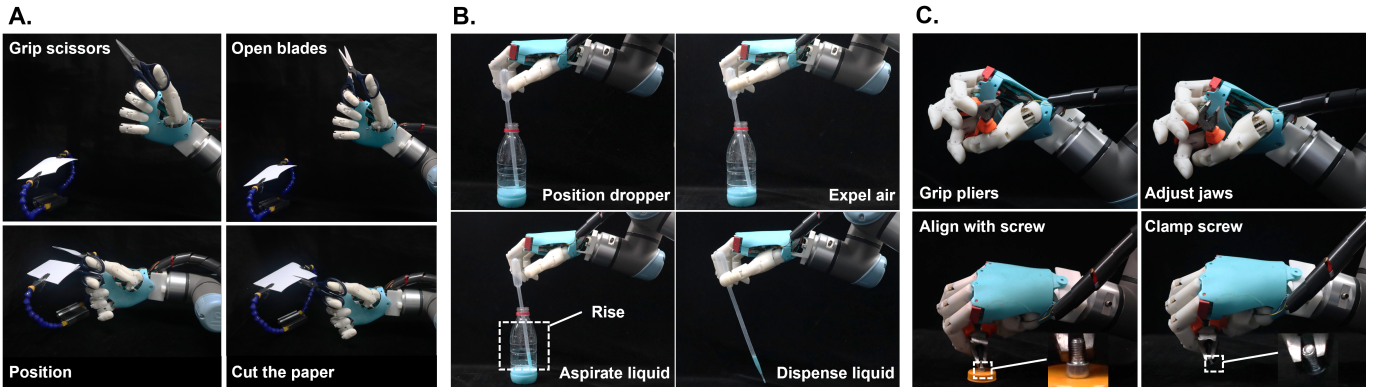


Fig. 8. Demonstration of dexterous hand manipulation capabilities through tool operations. (A) Shear paper with scissors. (B) Aspire liquid with a pipette. (C) Grip a screw with pliers.

IV. PERFORMANCE EVALUATION

In order to evaluate the performance of our proof-of-concept design, a series of experiments were conducted. The prototype hand, designed to emulate human dexterity and adaptability, was tested for its ability to grasp a variety of objects, perform in-hand manipulation, and operate tools for specific tasks.

A. Object Grasping and Manipulation

The grasping capability of the robotic hand, particularly in handling objects with varying shapes, weights, sizes, and thickness, serves as a crucial metric for evaluating its functionality. To comprehensively evaluate its performance, we selected a representative set of everyday objects as grasping targets. Drawing upon the established taxonomy of 33 valid grasp types identified by Feix [21], our investigation focused on six representative grasping modalities inspired by human grasping strategies: palm pinch, key pinch, spherical grip, two-finger lateral pinch, tip pinch, and cylindrical grip. Experimental results (Figure 7) demonstrate that the dexterous hand, through its anthropomorphic structural design and extensive

degrees of freedom, consistently achieved stable grasps across all selected objects while effectively replicating the functional versatility characteristic of human manual dexterity. These results highlight the hand’s remarkable adaptability to diverse object characteristics and its potential for practical applications when employing appropriate grasping strategies.

In-hand manipulation allows for the precise spatial adjustment of objects within the hand, thereby facilitating more effective grasping, placing, and subsequent operations. To realize this functionality in our dexterous robotic hand, motion data from the human hand was recorded and utilized to generate coordinated finger movement patterns. In the experiments, the hand grasped a pen using the middle and index fingers and adjusted its position through controlled flexion and lateral movements. Additionally, the hand achieved stable rotational manipulation of a cylindrical object (tape roll) while maintaining consistent contact pressure through precision pinch control. As illustrated in Figure 7, the results demonstrate the hand prototype’s capability to effectively reposition objects to desired locations through synchronized finger motion control. Quantitative analysis revealed that lateral movements are crit-

ical for ensuring grasping stability and positional accuracy in manipulation tasks.

B. Task-Oriented Tool Operation

The prototype hand was mounted on the UR5e robotic arm to evaluate its operational capabilities in practical tool manipulation scenarios. In the experiments, the hand executed complex tasks with everyday tools such as paper cutting, screw gripping, and liquid aspiration.

In the paper-cutting experiment, the dexterous hand demonstrated precise scissor manipulation by positioning the thumb and index finger on opposing handles. The coordinated movement of these two digits allowed the blades to open and close for cutting actions. Upon directing the scissors to the target position, the hand successfully cut through the paper with predetermined motions (Figure 8A). The liquid aspiration and transfer experiment highlighted the hand's force modulation capabilities. As illustrated in Figure 8B, the hand exhibited distinct force application patterns: higher fingertip forces were employed to expel air during the liquid aspiration phase, while maintaining optimal grip force during liquid transfer to prevent both slippage and premature liquid discharge. In the plier operation experiment, the hand securely gripped the plier's jaw with the thumb and index finger, while the ring and little fingers interlocked to firmly hold the handle. As shown in Figure 8 C, this configuration allowed for controlled jaw articulation through coordinated finger movements, effectively securing and lifting the screw from the desktop.

These experimental results demonstrate the prototype hand's functionality in tool manipulation and complex task execution. The hand exhibits versatile motion capabilities for intricate grasping patterns, effective tool operation, and precise force modulation, showcasing its potential for practical applications requiring dexterous manipulation and precise control.

V. CONCLUSION

In this study, we present a biomimetic, linkage-driven anthropomorphic hand designed to replicate the dexterity and adaptability of the human hand. Drawing upon the biomechanical principles of hand synergy, we developed a robotic hand featuring 19 joints driven by 11 active actuators. To achieve synergistic joint movements, we propose innovative planar and spatial linkage mechanisms with optimized geometric configurations. This design not only preserves the high degree of freedom required for intricate manipulation tasks but also ensures a compact and highly integrated structure. The experimental results demonstrate the prototype's exceptional performance in object grasping, in-hand manipulation, and tool operation, showcasing its potential for real-world applications. Future work will focus on enhancing the hand's sensory capabilities, refining control strategies, and exploring broader applications in prosthetics and humanoid robotics.

REFERENCES

[1] W. Townsend, "The barretthand grasper—programmably flexible part handling and assembly," *Industrial Robot: an international journal*, vol. 27, no. 3, pp. 181–188, 2000.

[2] W. Chen, Y. Wang, Z. Xiao, Z. Zhao, C. Yan, and Z. Li, "Design and experiments of a three-fingered dexterous hand based on biomechanical characteristics of human hand synergies," *IEEE/ASME Transactions on Mechatronics*, vol. 27, no. 5, pp. 2930–2941, 2021.

[3] U. Kim, D. Jung, H. Jeong, J. Park, H.-M. Jung, J. Cheong, H. R. Choi, H. Do, and C. Park, "Integrated linkage-driven dexterous anthropomorphic robotic hand," *Nature communications*, vol. 12, no. 1, pp. 1–13, 2021.

[4] J. N. Ingram, K. P. Körding, I. S. Howard, and D. M. Wolpert, "The statistics of natural hand movements," *Experimental brain research*, vol. 188, pp. 223–236, 2008.

[5] V. Gracia-Ibáñez, J. L. Sancho-Bru, M. Vergara, N. J. Jarque-Bou, and A. Roda-Sales, "Sharing of hand kinematic synergies across subjects in daily living activities," *Scientific reports*, vol. 10, no. 1, p. 6116, 2020.

[6] C.-H. Xiong, W.-R. Chen, B.-Y. Sun, M.-J. Liu, S.-G. Yue, and W.-B. Chen, "Design and implementation of an anthropomorphic hand for replicating human grasping functions," *IEEE Transactions on Robotics*, vol. 32, no. 3, pp. 652–671, 2016.

[7] B.-Y. Sun, X. Gong, J. Liang, W.-B. Chen, Z.-L. Xie, C. Liu, and C.-H. Xiong, "Design principle of a dual-actuated robotic hand with anthropomorphic self-adaptive grasping and dexterous manipulation abilities," *IEEE Transactions on Robotics*, vol. 38, no. 4, pp. 2322–2340, 2021.

[8] M. H. Chang, D. H. Kim, S.-H. Kim, Y. Lee, S. Cho, H.-S. Park, and K.-J. Cho, "Anthropomorphic prosthetic hand inspired by efficient swing mechanics for sports activities," *IEEE/ASME Transactions on Mechatronics*, vol. 27, no. 2, pp. 1196–1207, 2021.

[9] N. Karnati, B. A. Kent, and E. D. Engeberg, "Bioinspired sinusoidal finger joint synergies for a dexterous robotic hand to screw and unscrew objects with different diameters," *IEEE/ASME Transactions on Mechatronics*, vol. 18, no. 2, pp. 612–623, 2012.

[10] D. Yoon and Y. Choi, "Underactuated finger mechanism using contractible slider-cranks and stackable four-bar linkages," *IEEE/ASME Transactions on Mechatronics*, vol. 22, no. 5, pp. 2046–2057, 2017.

[11] K. Xu, J. Zhao, Y. Du, X. Sheng, and X. Zhu, "Design and postural synergy synthesis of a prosthetic hand for a manipulation task," in *2013 IEEE/ASME International Conference on Advanced Intelligent Mechatronics*. IEEE, 2013, pp. 56–62.

[12] J. Jin, W. Zhang, Z. Sun, and Q. Chen, "Lisa hand: Indirect self-adaptive robotic hand for robust grasping and simplicity," in *2012 IEEE International Conference on Robotics and Biomimetics (ROBIO)*. IEEE, 2012, pp. 2393–2398.

[13] H. Liu, K. Wu, P. Meusel, N. Seitz, G. Hirzinger, M. Jin, Y. Liu, S. Fan, T. Lan, and Z. Chen, "Multisensory five-finger dexterous hand: The dlr/hit hand ii," in *2008 IEEE/RSJ international conference on intelligent robots and systems*. IEEE, 2008, pp. 3692–3697.

[14] G. Li, X. Liang, Y. Gao, T. Su, Z. Liu, and Z.-G. Hou, "A linkage-driven underactuated robotic hand for adaptive grasping and in-hand manipulation," *IEEE Transactions on Automation Science and Engineering*, 2023.

[15] R. J. Schwarz and C. Taylor, "The anatomy and mechanics of the human hand," *Artificial limbs*, vol. 2, no. 2, pp. 22–35, 1955.

[16] M. Zarzoura, P. Del Moral, M. I. Awad, and F. A. Tolbah, "Investigation into reducing anthropomorphic hand degrees of freedom while maintaining human hand grasping functions," *Proceedings of the Institution of Mechanical Engineers, Part H: Journal of Engineering in Medicine*, vol. 233, no. 2, pp. 279–292, 2019.

[17] M. Laffranchi, N. Boccardo, S. Traverso, L. Lombardi, M. Canepa, A. Lince, M. Semprini, J. A. Saglia, A. Naceri, R. Sacchetti *et al.*, "The hannes hand prosthesis replicates the key biological properties of the human hand," *Science robotics*, vol. 5, no. 46, p. eabb0467, 2020.

[18] L. Birglen, "Type synthesis of linkage-driven self-adaptive fingers," 2009.

[19] H. Wang, S. Fan, and H. Liu, "Thumb configuration and performance evaluation for dexterous robotic hand design," *Journal of Mechanical Design*, vol. 139, no. 1, p. 012304, 2017.

[20] R. Abayasiri, R. Abayasiri, R. Gunawardhana, R. Premakumara, S. Mallikarachchi, R. Gopura, T. D. Lalitharatne, and D. Madusanka, "An under-actuated hand prosthesis with finger abduction and adduction for human like grasps," in *2020 6th International Conference on Control, Automation and Robotics (ICCAR)*. IEEE, 2020, pp. 574–580.

[21] T. Feix, J. Romero, H.-B. Schmiebmayer, A. M. Dollar, and D. Kragic, "The grasp taxonomy of human grasp types," *IEEE Transactions on human-machine systems*, vol. 46, no. 1, pp. 66–77, 2015.